

1 *Methods Paper*

## 2 **An Optimised GAS-pharyngeal cell biofilm model**

3 **Heema K. N. Vyas<sup>1,2</sup>, Jason D. McArthur<sup>2</sup>, Martina L. Sanderson-Smith<sup>1,2\*</sup>**

4 <sup>1</sup> Illawarra Health and Medical Research Institute, Wollongong, New South Wales, Australia.

5 <sup>2</sup> School of Chemistry and Molecular Bioscience, Molecular Horizons, University of Wollongong,  
6 Wollongong, New South Wales, Australia.

7 \* Correspondence: [martina@uow.edu.au](mailto:martina@uow.edu.au); Tel.: +61 2 42981935 (NSW, Australia)

8 Received: date; Accepted: date; Published: date

9 **Abstract:** Group A *Streptococcus* (GAS) causes 700 million infections and accounts for half a million  
10 deaths per year. Biofilm formation has been implicated in both pharyngeal and dermal GAS  
11 infections. *In vitro*, plate-based assays have shown that several GAS M-types form biofilms, and  
12 multiple GAS virulence factors have been linked to biofilm formation. Although the contributions  
13 of these plate-based studies have been valuable, most have failed to mimic the host environment,  
14 with many studies utilising abiotic surfaces. GAS is a human specific pathogen, and colonisation  
15 and subsequent biofilm formation is likely facilitated by distinct interactions with host tissue  
16 surfaces. As such, a host cell-GAS model has been optimised to support and grow GAS biofilms of  
17 a variety of GAS M-types. Improvements and adjustments to the crystal violet biofilm biomass assay  
18 have also been tailored to reproducibly detect delicate GAS biofilms. We propose 72 h as an optimal  
19 growth period for yielding detectable biofilm biomass. GAS biofilms formed are robust and durable,  
20 and can be reproducibly assessed via staining/washing intensive assays such as crystal violet with  
21 the aid of methanol fixation prior to staining. Lastly, SEM imaging of GAS biofilms formed by this  
22 model are resemblant of those previously found on excised tonsils of patients suffering chronic  
23 pharyngo-tonsillitis. Taken together, we outline an efficacious GAS biofilm pharyngeal cell model  
24 that can support long-term GAS biofilm formation, with biofilms formed closely resembling those  
25 seen *in vivo*.

26 **Keywords:** Group A *Streptococcus*; *Streptococcus pyogenes*; biofilm; host-pathogen; pharyngeal;  
27 biofilm modelling

28

---

## 29 **Introduction**

30 *Streptococcus pyogenes* (Group A *Streptococcus*; Group A streptococci; GAS) is a Gram-positive  
31 human pathogen known to cause an array of infections ranging from mild infections of the skin and  
32 throat, to more serious and life threatening conditions such as necrotising fasciitis and numerous  
33 autoimmune sequelae [1]. GAS infections are a considerable burden on global healthcare systems  
34 with high rates of patient mortality and morbidity [2].

35 GAS has been found to form biofilms in the tonsillar crypts of patients with GAS pharyngitis  
36 and in the skin lesions of GAS impetigo sufferers [3,4]. *In vitro*, it has been demonstrated that GAS  
37 biofilm formation is strain dependent. And among isolates of the same serotype, biofilm forming  
38 capacities are oftentimes found to differ considerably [5]. As highlighted in Table 1, *in vitro* plate-  
39 based studies have implicated several GAS virulence factors (M protein, capsule, pili, SpeB, CovS,  
40 and quorum sensing peptides) in biofilm formation [6]. These findings have contributed substantially  
41 to our current understanding of GAS biofilms and their involvement in GAS pathogenesis and  
42 disease. However, much of this work has been conducted on abiotic surfaces (plastic, glass, and  
43 silicone). To date, few studies have used host matrix components like collagen, fibronectin, or  
44 fibrinogen as surface coatings for GAS biofilm studies [7-10]. Moreover, there is currently no  
45 methodology or protocol widely recognised as the gold standard for GAS biofilm formation. The  
46 variability among methods, and limited use of host factors in *in vitro* plate-based GAS biofilm models  
47 found in previous studies has been summarised in Table 1. This table highlights that only three *in*  
48 *vitro* plate-based studies utilising epithelial monolayers to grow and support GAS biofilms have been  
49 published.

50 There is a need for GAS biofilm models to better incorporate host factors, as it has been found  
51 that failure to do so has significant effects on the biofilms formed, with the overall arrangement and

52 architecture of biofilms and their virulence gene expression, found to noticeably differ from that of  
53 biofilms formed *in vivo* [10]. Moreover, tissue tropism displayed by differing GAS isolates towards  
54 the throat and skin, which are vastly different epithelial landscapes and environments [11], will  
55 influence GAS adherence, colonisation, and subsequent biofilm formation. Thus, the incorporation  
56 of relevant host epithelial substratum, and an overall mimicking of the host environment should be  
57 a consideration in GAS biofilm modelling.

58 Here, a GAS-pharyngeal cell biofilm model has been optimised to cultivate robust GAS biofilms  
59 that can be used for a diverse set of GAS M-types. We also present optimised steps and tips for  
60 increased biofilm integrity and reproducibility when performing staining assays like crystal violet.  
61 This model has since been used to effectively assess the role pharyngeal cell surface glycans play in  
62 GAS biofilm formation and clearly demonstrates the importance of mimicking the epithelial  
63 environment in these studies [12].

**Table 1. Examples of *in vitro* plate-based models used for the study of GAS biofilm formation.**

Growth Substratum	Time	Media conditions	Inoculum*	<i>emm</i> -type	Purpose of the study	Ref.
Polystyrene	Up to 96 h	C medium, 23°C	0.1:10	<i>emm14</i>	Biofilm forming abilities of WT GAS compared to mutants (capsule, <i>mga</i> virulence regulon, M-protein, and <i>covR</i> )	[10]
Polystyrene	24 h	THY - 0.2% yeast supplemented with 0.5% glucose, 37°C	1:100	<i>emm14</i>	Microcolony-dependent and -independent biofilm formation, with a focus on the role of GAS capsule	[13]
Glass and cellular form of fibronectin (cFn) coated glass	1 or 24 h	Brain heart infusion (BHI) and THY + 0.2% yeast, 37°C	Exponential phase GAS	<i>emm1</i> , 28, and 41	Streptococcal collagen-like protein-1 (Scl1) binding wound associated cFn (with extra domain A) involvement in biofilm formation	[7]
Human: fibronectin, fibrinogen, laminin, collagen coated, or uncoated polystyrene	12 to 120 h	Luria Broth, THY - 0.5% yeast, BHI, or chemically defined medium, 37°C	1x10 <sup>4</sup> CFU/ml	<i>emm1</i> , 2, 3, 6, 12, 14, 18, 28, and 49  <i>emm14</i> and <i>emm18</i>	Effect of coating with human matrix components in potentiating biofilm formation.  Investigating quorum sensing signaling peptide SiC in mediating biofilm density and structure	[8]
Polylysine coated glass coverslips	72 h	C medium, 37°C	1:10		Pilli involvement in mature biofilm formation	
Pharyngeal: Detroit 562 monolayers	2 h	THY, 37°C	0.6 OD <sub>600nm</sub>	<i>emm1</i>	Pilli involvement in initial adhesion and its role in microcolony development	[14]
Pharyngeal: Detroit 562 monolayers	72 h	THY, 34°C	1:20	<i>emm1</i> , 3, 9, 12, 44, 53, 90, 98, 108	Assessing the role of pharyngeal cell surface glycans in GAS biofilm formation in the context of GAS pharyngitis	[12]
Skin: SCC13 monolayers cells	48 h	THY- 0.5% yeast, 34°C	2 x 10 <sup>4</sup> CFU/0.5mL	<i>emm3</i> and <i>emm6</i>	Biofilms examined for colonisation, virulence, and genetic diversity	[15]

\*Inoculums listed as ratios (bacteria: bacterial media), growth phase, or optical density.

## 66 Materials and Methods

### 67 GAS and culture conditions

68 GAS strains used in this study (Table 2) are clinical GAS isolates, with each strain representative  
69 of a discrete GAS *emm*-type [16-18]. GAS was grown on horse blood agar (HBA) plates (Oxoid, UK) or  
70 Todd Hewitt agar supplemented with 1% (w/v) yeast (THYA) (Difco, Australia). Static cultures of GAS  
71 were grown overnight in Todd Hewitt broth supplemented with 1 % (w/v) yeast (THY). GAS was  
72 cultured, maintained, and biofilms formed at 34°C to mimic conditions more closely seen in the *in vivo*  
73 pharyngeal environment as described by Marks, *et al.* [19].

74 **Table 2. GAS strains utilised in this study, their *emm*-types, and clinical source.**

M-type	Strain	Clinical source	Ref.
M1	5448	Invasive infection: Necrotising fasciitis and toxic shock	[18]
M12	PRS-8	Superficial infection: persistent Pharyngeal pus/sinusitis	[17]
M3	90254	Invasive infection	[17]
M98	NS88.2	Invasive infection: Blood (bacteraemia)	[16]
M108	NS50.1	Superficial infection: Wound	[16]

### 75 Human pharyngeal cell culture conditions

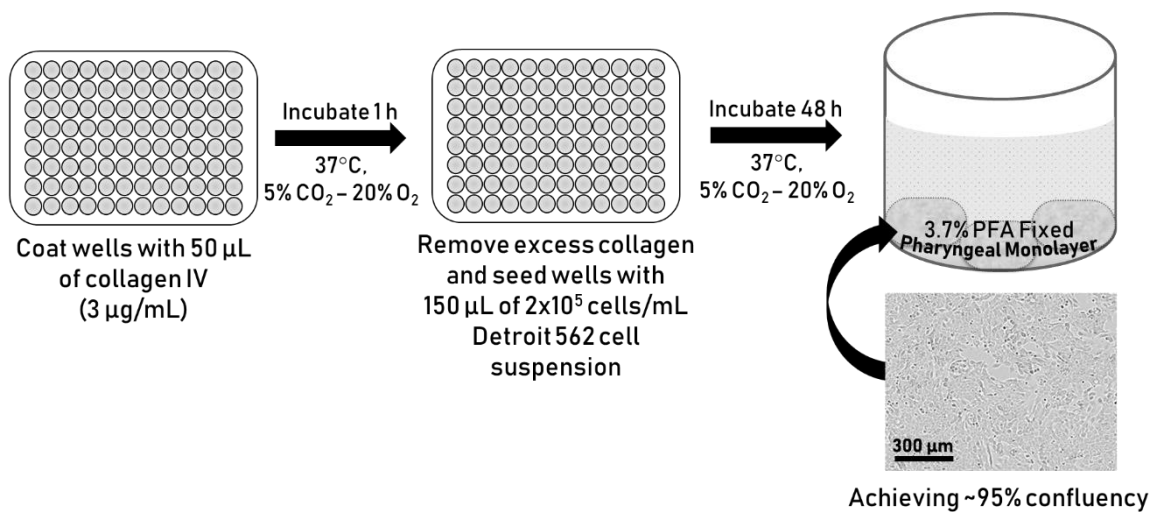
76 Detroit 562, a human pharyngeal epithelial cell line (CellBank Australia, Australia), was cultured  
77 in Dulbecco's Modified Eagle Medium (DMEM) F12 (Invitrogen, Australia), supplemented with 2 mM  
78 L-glutamine (Gibco, Life Technologies, UK) and 10 % (v/v) heat inactivated foetal bovine serum (FBS)  
79 (Bovogen Biologicals, Australia) in cell culture flasks at 37°C, 5% CO<sub>2</sub>– 20% O<sub>2</sub> atmosphere.

### 80 Pharyngeal cell monolayer formation

81 Detroit 562 pharyngeal cell monolayers form the substratum for GAS biofilm growth. An outline  
82 of the process and the monolayers formed is depicted in Fig. 1.

- 83 • The wells of a 96-well flat bottom cell culture microtiter plate (Greiner Bio-One, Germany) were  
84 coated with 50 µL of 300 µg/mL Collagen I from rat tail (Gibco, Life Technologies, UK)  
85 prepared in pre-chilled, sterile 17.4 mM acetic acid solution. The plate was incubated for 1 h,  
86 37°C, 5% CO<sub>2</sub>– 20% O<sub>2</sub> atmosphere.

- 87
- After 1 h, excess collagen was removed, and the wells seeded with 150  $\mu$ L Detroit 562 cell
- 88 suspension ( $2 \times 10^5$  cells/mL) and cultured for 48 h (to achieve ~95% confluency).
- 89
- Monolayers were washed once with 200  $\mu$ L of sterile PBS, and fixed with 50  $\mu$ L sterile 3.7%
- 90 paraformaldehyde (PFA) (w/v) for 20 min.
- 91
- Once cells were fixed, PFA was removed and wells washed twice with 200  $\mu$ L of PBS.
- 92
- Monolayers can be used immediately, or stored at 2-8°C for up to two weeks (with monolayers
- 93 kept wet via submersion in 200  $\mu$ L of sterile PBS) until required for use.



94 **Figure 1. Schematic outlining the process of Detroit 562 pharyngeal cell monolayer formation.**

95 Schematic shows collagen coating, seeding with Detroit 562 pharyngeal cells, and finally an example

96 well containing a 3.7% PFA fixed ~95% confluent monolayer of Detroit 562 pharyngeal cells. Example

97 monolayer image taken at 10x objective at the Incucyte.

#### 98 *GAS biofilm formation*

- 99
- Wells containing pre-formed fixed Detroit 562 pharyngeal cell monolayers were seeded with
- 100 150  $\mu$ L of overnight GAS culture diluted 1:20 in THY-glucose (0.5% glucose v/v) (THY-G).
- 101 Wells containing 150  $\mu$ L sterile THY-G (no bacteria) served as media sterility controls and
- 102 blanks.
- 103
- The plate was incubated for 2 h (34°C, 50 rpm) to facilitate GAS interacting with and adhering
- 104 to the pharyngeal cell monolayer substratum.

- 105           ○ *Tips to avoid evaporation from the biofilm plate:*
- 106                     ▪ *Peripheral wells can evaporate quickly, and in turn this affects the biofilms grown and*
- 107                                 *subsequently assayed. Thus, it is advised (where possible) to grow biofilms in the*
- 108                                 *inner-most wells of the plate, with wells not in use filled with 200  $\mu$ L of sterile water.*
- 109                     ▪ *Secondly, store plates in a sealed container filled with water to further avoid*
- 110                                 *dehydration of biofilm wells within the plate.*
- 111                                 · *Mount on an appropriate stage to keep plate elevated well above water level.*
- 112         • At 2 h, non-adherent GAS were removed and wells replenished with 150  $\mu$ L of sterile THY-G.
- 113         Note: The current protocol was designed to model biofilms formed following the initial
- 114         interaction occurring between GAS-host cell surface structures at the 2 h point. Thus, this
- 115         incubation time can be changed dependent on the nature of the study.
- 116         • THY-G media was refreshed every 24 h to remove old media containing planktonic/loosely
- 117         bound cells, debris, and any waste. Note: GAS biofilms are quite delicate.
- 118           ○ *Tips for media changing:*
- 119                     ▪ *The pipette tip should be placed just below the meniscus of the media, and firmly*
- 120                                 *against the wall of the well at an angle of  $\sim 45^\circ$ .*
- 121                     ▪ *To change media with minimal disruption to the biofilm, it is best to remove and*
- 122                                 *replenish the THY-G media slowly and gradually (swapping out 50  $\mu$ L at a time).*
- 123                                 · *Together, this reduces any biofilm disruption/dislodgement.*
- 124         • At 72 h, mature and robust GAS biofilms are produced.

## 125 GAS biofilm biomass crystal violet staining

126 Biofilm biomass is assayed via crystal violet staining.

- 127         • Biofilms were thoroughly air dried for 30-40 mins (or until fully dried)
- 128           ○ *Tip: When completely removing media, adjust the pipetting volume (e.g.  $\sim 145 \mu$ L) to account*
- 129                                 *for any media loss due to evaporation. This prevents/reduces biofilm disruption/loss into pipette*
- 130                                 *tip.*

- 131 • Dried biofilms were then fixed with 150  $\mu$ L of 99% methanol for 15 min.
- 132     ○ *Tip: Fix with closed lid to minimise methanol evaporation.*
- 133 • Once fixed, the methanol was gently and slowly removed from the biofilms
- 134     ○ *Tip: Given methanol's propensity to evaporate, pipetting volume adjustment (e.g. ~145  $\mu$ L) is*
- 135     *recommended. This prevents/reduces biofilm disruption/loss into the pipette tip.*
- 136 • Biofilms were thoroughly air-dried and stained with 150  $\mu$ L of 0.2% crystal violet (w/v) (Sigma-
- 137 Aldrich, USA) supplemented with 1.9% ethanol (v/v) for 10 min (RT, static).
- 138     ○ Monolayers with THY (no GAS biofilm) served as media sterility controls and
- 139     background staining controls, with absorbance values subtracted from those of
- 140     biofilm samples.
- 141 • Once stained, excess crystal violet was removed, and biofilms gently washed twice with 200
- 142  $\mu$ L of PBS.
- 143 • Crystal violet stain that had incorporated into the biofilm was re-solubilised upon the addition
- 144 of 150  $\mu$ L of 1% sodium dodecyl sulphate (SDS) (w/v) (Sigma-Aldrich, USA).
- 145     ○ Plate was incubated for 10 min (RT, static).
- 146 • Biofilm biomass was quantified spectrophotometrically at OD<sub>540nm</sub> (SpectraMax Plus 384
- 147 microplate reader).

#### 148 *Scanning Electron Microscopy*

149 Scanning electron microscopy (SEM) was utilised to image M1, M12, and M3 GAS biofilms formed

150 on the Detroit 562 pharyngeal cell monolayers as these are all associated with GAS pharyngitis [1].

151 Preparation of biofilms for SEM was adapted from [20] with the following modifications.

- 152 • M1 and M12 GAS biofilms were grown on Detroit 562 pharyngeal cell monolayers previously
- 153 pre-formed on 13 mm plastic Nunc Thermanox coverslips (Proscitech, USA) in a 12-well
- 154 polystyrene plate.



- 155 • Biofilms were air dried, and pre-fixed in 2.5% glutaraldehyde, 50 mM L-lysine  
156 monohydrochloride, and 0.001% ruthenium red solution prepared in 0.1 M HEPES buffer (pH  
157 7.3) (30 min, 4°C).
- 158 • Following pre-fixation, biofilms were fixed in fixative solution (2.5% glutaraldehyde and  
159 0.001% ruthenium red prepared in 0.1 M HEPES buffer, pH 7.3) for 1.5 h (4°C) and washed  
160 twice in 0.1M HEPES buffer.
- 161 • 2% osmium tetroxide vapour was used post-fixation (2 h) followed by three washes with  
162 distilled water (each 15 mins).
- 163 • A graded ethanol series (30%, 50%, 70%, 90%, and 3x 100%) was then used to remove all water  
164 from the biofilms before they were critical point dried (Leica CPD 030, Austria).
- 165 • Dried biofilms were then sputter coated with 20 nm platinum (Edwards Vacuum coater, USA)  
166 and visualised using a JEOL JSM-7500 microscope (JEOL, Japan) at 500, 5000, and 15 000 x  
167 magnification.
- 168 • Detroit 562 pharyngeal monolayer controls (without biofilms) were also imaged at 500 and  
169 5000 x magnification.
- 170 • Images were taken at random positions within the samples by a UOW Electron Microscopy  
171 Centre technician blinded from the study in an effort to reduce bias.

## 172 *Statistical Analysis*

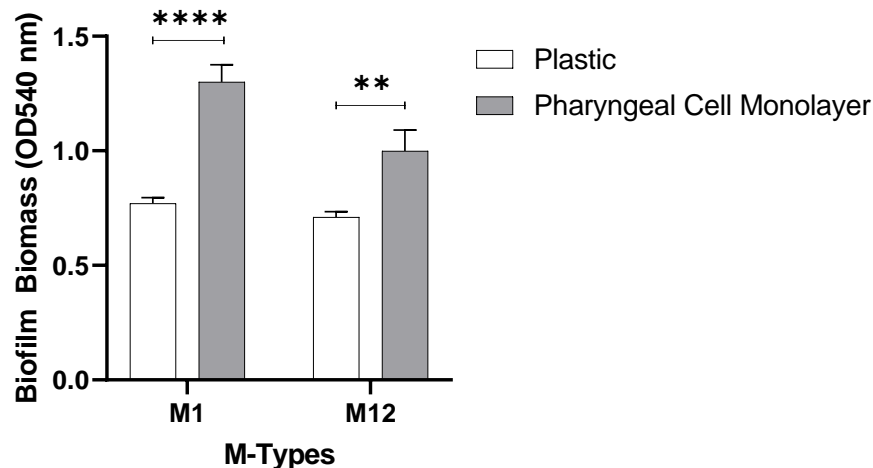
173 All statistical analysis was performed using GraphPad Prism (version 8.4.0, GraphPad Software,  
174 USA). Datasets were compared using a student T-test, and a P-value of  $\leq 0.05$  was considered  
175 significant.

## 176 **Results**

### 177 *48 h GAS biofilms are potentiated on Detroit 562 pharyngeal cell monolayers*

178 To exemplify and highlight the need for a more physiologically relevant substratum for GAS  
179 biofilm growth, two commonly studied GAS isolates, M1 (5448) and M12 (PRS-8), implicated in GAS

180 pharyngitis were assessed and were the primary focus of this study [1]. Specifically, 48 h M1 and M12  
181 GAS biofilms were assessed for their biofilm forming abilities on both a plastic substratum and  
182 Detroit 562 pharyngeal cell monolayers via crystal violet staining (Fig. 2). Both GAS M-types were  
183 found to exhibit significantly greater biofilm biomass when grown on the Detroit 562 pharyngeal cell  
184 monolayers.



185 **Figure 2. M1 and M12 GAS were assessed for the ability to form biofilm on plastic and Detroit 562**  
186 **pharyngeal cell monolayers.** 48 h biofilms were formed and biofilm biomass ascertained via crystal  
187 violet staining. Monolayers with THY (no GAS biofilm) served as media sterility controls and  
188 background staining controls, with absorbance values subtracted from those of biofilm samples. Data  
189 represents mean  $\pm$  SEM, \*\* ( $P \leq 0.01$ ) and \*\*\*\* ( $P \leq 0.0001$ );  $n = 3$  biological replicates, with 3 technical  
190 replicates each.

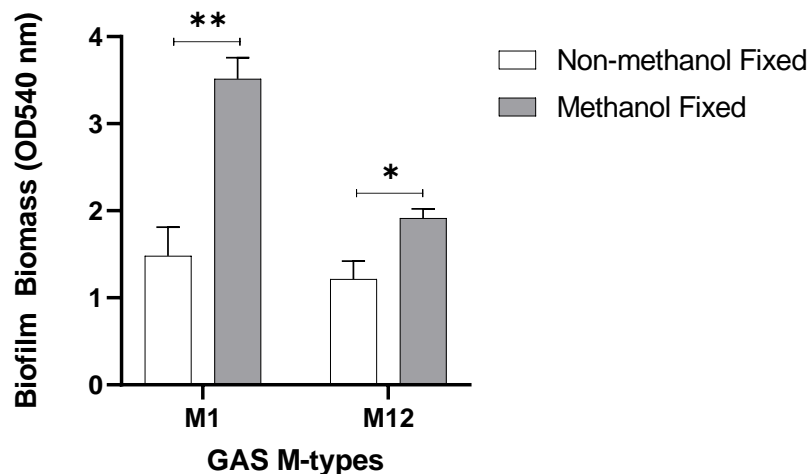
191 *Methanol fixation improves reproducibility of crystal violet staining on GAS biofilms*

192 Crystal violet assays were first described by Christensen, *et al.* [21] as a means of quantifying  
193 biofilm. Crystal violet has proven useful in that it detects biofilm in its entirety, staining a biofilms  
194 biomass which comprises live and dead cells, as well as EPS matrix. Taken together with its overall  
195 ease of use and relatively low cost it has since become a routinely used biofilm stain and detection  
196 method [22]. Despite these attributes, there are some drawbacks and limitations to crystal violet use,  
197 with concerns around reproducibility [23,24]. Reproducibility can be influenced by a biofilms overall  
198 durability and stability, especially during the wash steps [24]. As such, biofilms that are thinner and  
199 flimsier require further consideration of overall biofilm handling. Additional steps to the crystal

200 violet assay can be implemented to ensure biofilm retention during the various washing, staining,  
201 and de-staining steps of the assay.

202 In the current study, to minimise disruption and damage to the biofilm, biofilm plate  
203 layout/growth conditions and overall handling were optimised as outlined in the methods according  
204 to the following specifications; growing biofilms at the inner-most wells of a plate with unused wells  
205 filled with water to avoid dehydration; adjusting pipetting volume for media removal to account for  
206 dehydration during incubations; placing the plate inside a container containing additional water to  
207 reduce media evaporation from the wells; gradual media changes (50  $\mu$ L at a time, as opposed to the  
208 entire 150  $\mu$ L) etc. Furthermore, to improve the durability of the biofilms during crystal violet  
209 assaying, 48 h biofilms grown on the Detroit 562 pharyngeal monolayers were either fixed with  
210 methanol or left unfixed and assessed for biofilm biomass (Fig. 3).

211 Methanol fixation was found to significantly increase retention of biofilm biomass following  
212 crystal violet staining (Fig. 3). Hence, for GAS biofilms, we recommend methanol fixation as an  
213 additional step prior to crystal violet staining.

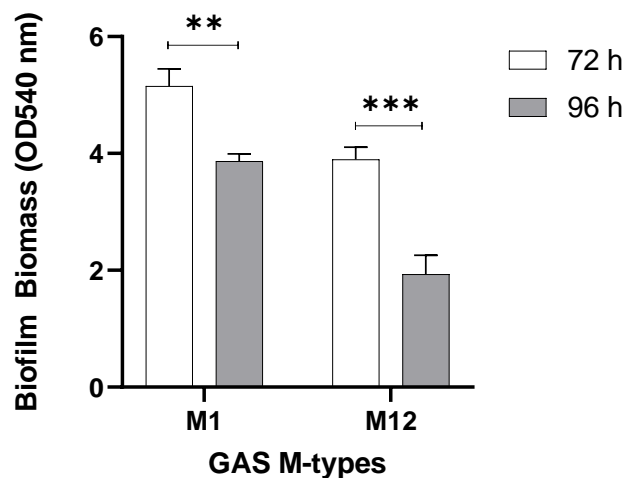


214 **Figure 3. Methanol fixation improves M1 and M12 GAS biofilm biomass detection.** 48 h GAS  
215 biofilms were formed from planktonic GAS that had initially adhered to the Detroit 562 pharyngeal  
216 cell monolayer after 2 h incubation. Biofilm biomass was ascertained via crystal violet staining.  
217 Monolayers with THY (no GAS biofilm) served as media sterility controls and background staining  
218 controls, with absorbance values subtracted from those of biofilm samples. Data represents mean  $\pm$   
219 SEM, \* ( $P \leq 0.05$ ) and \*\* ( $P \leq 0.01$ );  $n = 3$  biological replicates, with 3 technical replicates each.

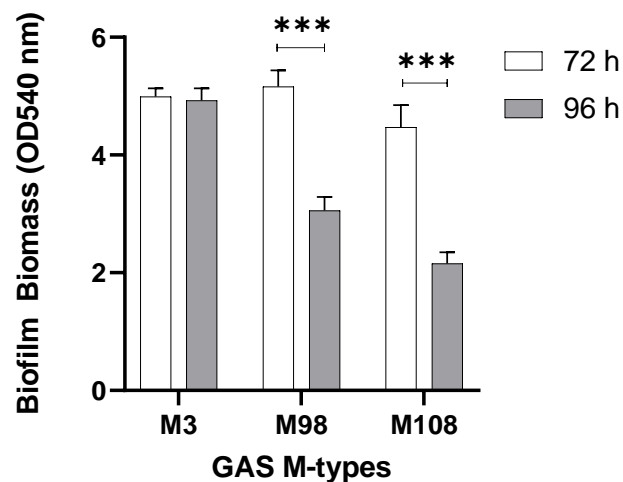
220 72 h growth yields optimal biofilm biomass

221 After optimising the crystal violet assay for GAS biofilms, M1 and M12 GAS biofilm formation  
222 on the Detroit 562 pharyngeal cell monolayers was further assessed at extended growth periods of  
223 72 and 96 h to see if greater biofilm biomass was achievable (Fig. 4). Both M1 and M12 formed  
224 significantly more biofilm at 72 h compared to 96 h where biofilm biomass seemed to diminish. The  
225 biofilm biomass at 72 h was also greater than the biofilm biomass formed previously at 48 h.

226 To build upon this and assess the utility of the optimised methodology, additional GAS M types  
227 (M3 (90254), M98 (NS88.2), and M108 (NS50.1)) were also assayed for biofilm formation under the  
228 same conditions (Fig. 5). As per M1 and M12, both M98 and M108 formed significantly greater biofilm  
229 at 72 h compared 96 h. However, biofilm biomass remained relatively unchanged for M3 at both 72  
230 h and 96 h growth periods.



231 **Figure 4. 72 h is an optimal period for GAS biofilm formation.** M1 and M12 were assessed for GAS  
232 biofilm formation at 72 and 96 h. 72 h yielded significantly more biofilm than 96 h. Biofilm biomass  
233 was determined via crystal violet staining. Monolayers with THY (no GAS biofilm) served as media  
234 sterility controls and background staining controls, with absorbance values subtracted from those of  
235 biofilm samples. Data represents mean  $\pm$  SEM, \*\* ( $P \leq 0.01$ ) and \*\*\* ( $P \leq 0.001$ );  $n = 3$  biological  
236 replicates, with 3 technical replicates each.

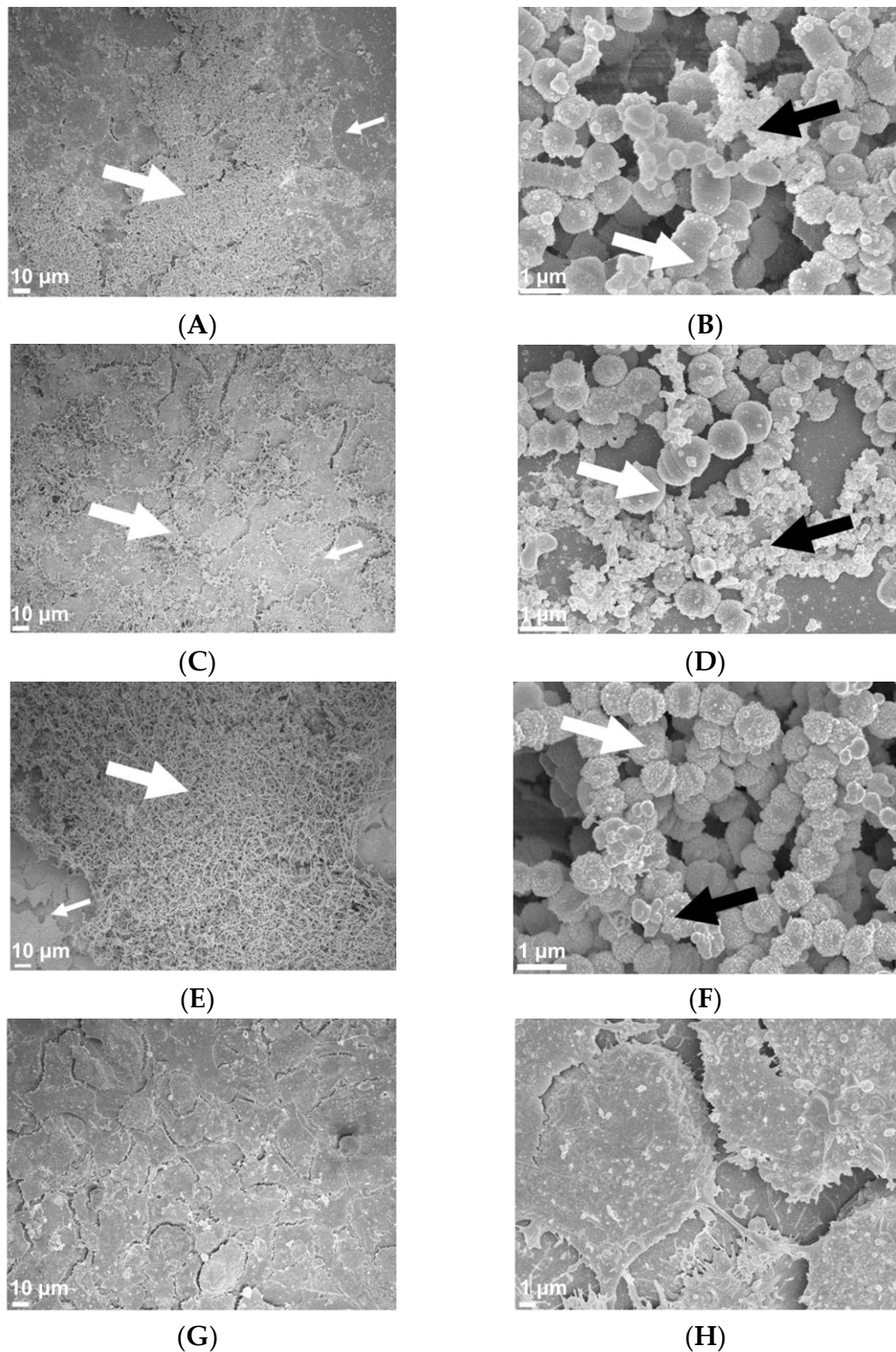


237 **Figure 5. Assessing the utility of the optimised methodology on additional GAS M types (M3, 98,**  
238 **and 108).** Biofilm biomass was determined via crystal violet staining. Monolayers with THY (no GAS  
239 biofilm) served as media sterility controls and background staining controls, with absorbance values  
240 subtracted from those of biofilm samples. Data represents mean  $\pm$  SEM, \*\* ( $P \leq 0.01$ ) and \*\*\* ( $P \leq 0.001$ );  
241  $n = 3$  biological replicates, with 3 technical replicates each.

242 *SEM imaging reveals 72h M1, M12, and M3 GAS biofilms formed in the host cell-GAS model closely*

243 *resemble those in vivo*

244 M1 and M12, as well as an M3 strain also implicated in GAS pharyngitis [1] was imaged via  
245 SEM. Specifically, 72 h GAS biofilms grown on Detroit 562 pharyngeal cell monolayers were visually  
246 observed by SEM for their overall biofilm architecture, arrangement, and structure. M1, M12, and M3  
247 GAS biofilms show cocci chains arranged in three-dimensional aggregated communities atop the  
248 Detroit 562 pharyngeal cell monolayers (Fig 6). However, M1 (Fig. 6 A and B) and M3 (Fig. 6 E and  
249 H) biofilms were found to arrange in tightly packed aggregates of cocci chains on the Detroit 562  
250 monolayers, whereas M12 biofilms were more loosely arranged atop of the monolayers (Fig. 6 C and  
251 D). All biofilms produced noticeable EPS that was found closely associated with the cocci chains (Fig  
252 6. B, D, and F). Detroit 562 pharyngeal cell monolayers (without biofilm) are also shown (Fig 6. G and  
253 H) depicting the pharyngeal cells arranged in confluent monolayers, with pharyngeal cells displaying  
254 their cell surface projections.



255  
256  
257  
258  
259  
260

**Figure 6. Representative 72 h M1 (A and B), M12 (C and D), and M3 (E and F) GAS biofilms visualised by scanning electron microscopy at 500 and 15 000 x magnification. GAS biofilms show chained cocci (white arrows) arranged into three dimensional aggregated structures with EPS (black arrows) upon the Detroit 562 monolayers (smaller white arrows). Detroit 562 monolayers (without biofilm) (G and H) were also imaged at 500 and 5000 x magnification. Images represent 3 biological replicates, with 3 technical each.**



## 261 Discussion

262 GAS is a human pathogen, which when in the host is reliant on several host factors to prompt  
263 and facilitate dynamic and unique interactions necessary for successful colonisation and persistence.  
264 Most *in vitro* plate-based GAS biofilm models used previously do not mimic the host environment.  
265 Moreover, the use of an epithelial substratum for growth is rare. Given the importance of the GAS-  
266 host tissue interface in mediating the earlier stages of GAS association and adherence, it is likely that  
267 these interactions are also crucial for various stages of subsequent biofilm formation and  
268 establishment within the host. Thus, modelling in the absence of host factors and/or relevant host  
269 epithelial substratum in *in vitro* plate-based biofilm models may result in biofilms that do not  
270 accurately represent the GAS biofilms *in vivo*. Here we report an optimised method for GAS biofilm  
271 formation using Detroit 562 pharyngeal cell monolayers as a model for GAS-host interaction.

272 In the current study, an optimised method for forming GAS biofilm on fixed pharyngeal cell  
273 monolayers has been developed. Despite Detroit 562 pharyngeal cells not being a primary cell line,  
274 they are suitable for this model for numerous reasons; i) the cell line is derived directly from human  
275 pharyngeal tissue, a site which GAS readily colonises, ii) retention of surface structures after culturing  
276 for adherence (e.g. carbohydrate epitopes) representative of native pharyngeal cells has been noted,  
277 and iii) they have been used extensively in planktonic GAS adherence assays [11,25-28]. Overall,  
278 utilisation of pharyngeal epithelial substratum within this model aimed to better recreate the host  
279 environment than in most of the *in vitro* models used previously.

280 GAS biofilm biomass increased significantly when grown on fixed Detroit 562 pharyngeal cell  
281 monolayers, when compared to biofilm grown on abiotic plastic substratum. This highlights the  
282 difference in biofilm potentiation, as a direct result of substratum for biofilm growth. This supports  
283 the utility for GAS biofilm modelling to include epithelia as a substratum for biofilm growth over an  
284 abiotic plastic surface. Whilst various staining techniques have been developed to assess biofilm  
285 biomass, crystal violet staining remains one of the most common techniques within the field. Here,  
286 we propose optimisation of this method at the biofilm formation steps preceding crystal violet

287 staining, as well as additional considerations required during the crystal violet assay that are tailored  
288 to the GAS biofilms formed using this model. Specifically, to further improve biofilm detection,  
289 durability, and subsequent reproducibility of the commonly used biofilm biomass crystal stain assay,  
290 methanol fixation was assessed. 48 h GAS biofilms that were methanol fixed prior to crystal violet  
291 staining yielded greater biofilm biomass, with less biofilm loss during the intensive staining and  
292 washing steps. In turn, reducing error, and increasing reproducibility.

293 Broth grown GAS is inherently toxic to epithelial cells, as such, there have previously been no  
294 models that explore or support long-term GAS biofilm-epithelia co-culture in a plate-based model  
295 [15]. Here, we show that fixed pharyngeal cell monolayers support GAS biofilm formation beyond  
296 48 h. However, of the three time points assessed, 72 h is the most optimal biofilm growth period for  
297 yielding the greatest biofilm biomass for M1, M12, M98, and M108 GAS. Biofilm biomass was seen  
298 to diminish at 96 h, likely resulting from partial disintegration of biofilm. This may be indicative of a  
299 mature or older biofilm reaching the final step of the biofilm life cycle - dispersal. Dispersal is thought  
300 to be triggered by nutrient exhaustion at the site, which in a host enables bacteria to shift to a motile  
301 planktonic state for biofilm re-establishment elsewhere [8,29,30]. These results agreed with a previous  
302 study of M6 and M49 biofilms grown on abiotic plastic well surfaces of a 96 well plate-based system,  
303 whereby biofilms had greater biomass at 72 h, and exhibited partial disintegration at 96 h with  
304 authors attributing this to the age of the biofilm and nutrient limitation [8].

305 Finally, visual inspection of the GAS biofilms via SEM imaging found M1, M12, and M3 formed  
306 biofilm atop the Detroit 562 pharyngeal cell monolayers. Cocci chains, typical of GAS, can be seen  
307 arranged in three dimensional aggregated structures coated in EPS matrix for all three M-types.  
308 Importantly, biofilms formed in this GAS-pharyngeal epithelial cell model appear similar to SEM  
309 images captured of GAS biofilms found at the surface of tonsils removed from patients with recurrent  
310 GAS tonsillo-pharyngitis [3].

311 Here we demonstrate an efficacious GAS biofilm-pharyngeal cell model that can support long-  
312 term biofilm formation, with biofilms formed resembling those seen *in vivo*. This model has since



313 been used for assessing the role of pharyngeal cell surface glycans in mediating GAS biofilm  
314 formation [12]. Hence, the value of this model is that it can be used to explore a plethora of  
315 interactions occurring at the GAS-host cell surface interface and the subsequent effects these  
316 interactions exert on biofilm formation.

317 **Author Contributions statement:** Conceptualisation, H.K.N.V, M.L.S-S, and J.D.M; methodology, H.K.N.V;  
318 formal analysis, H.K.N.V; investigation, H.K.N.V; resources, M.L.S-S, and J.D.M; data curation, H.K.N.V;  
319 writing—original draft preparation, H.K.N.V; writing—review and editing, H.K.N.V, M.L.S-S, and J.D.M;  
320 visualisation, H.K.N.V; supervision, M.L.S-S, and J.D.M; funding acquisition, M.L.S-S and J.D.M. All authors  
321 have read and agreed to the published version of the manuscript.

322 **Funding:** This work was funded by an NHMRC Project Grant APP1143266 and Molecular Horizons to M.L.S-S.  
323 H.K.N.V is a recipient of an Australian Postgraduate Award.

324 **Acknowledgments:** The authors acknowledge the valuable assistance of staff at the UOW Electron Microscopy  
325 Centre for their help with the specimen preparation and the operation of the JEOL 7500 SEM. We also thank  
326 Emma Jayne-Proctor for her technical support.

327

#### 328 **Additional Information**

329 **Competing interests' statement:** The authors declare no conflict of interest.

#### 330 **References**

- 331 1. Walker, M.J.; Barnett, T.C.; McArthur, J.D.; Cole, J.N.; Gillen, C.M.; Henningham, A.;  
332 Sriprakash, K.S.; Sanderson-Smith, M.L.; Nizet, V. Disease Manifestations and Pathogenic  
333 Mechanisms of Group A Streptococcus. *Clinical Microbiology Reviews* **2014**, *27*, 264-301,  
334 doi:10.1128/CMR.00101-13.
- 335 2. Carapetis, J.R.; Steer, A.C.; Mulholland, E.K.; Weber, M. The global burden of group A  
336 streptococcal diseases. *The Lancet infectious diseases* **2005**, *5*, 685-694.
- 337 3. Roberts, A.L.; Connolly, K.L.; Kirse, D.J.; Evans, A.K.; Poehling, K.A.; Peters, T.R.; Reid, S.D.  
338 Detection of group A Streptococcus in tonsils from pediatric patients reveals high rate of  
339 asymptomatic streptococcal carriage. *BMC Pediatrics* **2012**, *12*, 3-3, doi:10.1186/1471-2431-12-  
340 3.
- 341 4. Akiyama, H.; Morizane, S.; Yamasaki, O.; Oono, T.; Iwatsuki, K. Assessment of Streptococcus  
342 pyogenes microcolony formation in infected skin by confocal laser scanning microscopy.  
343 *Journal of Dermatological Science* **2003**, *32*, 193-199, doi:[http://dx.doi.org/10.1016/S0923-  
344 1811\(03\)00096-3](http://dx.doi.org/10.1016/S0923-1811(03)00096-3).
- 345 5. Baldassarri, L.; Creti, R.; Recchia, S.; Imperi, M.; Facinelli, B.; Giovanetti, E.; Pataracchia, M.;  
346 Alfarone, G.; Orefici, G. Therapeutic failures of antibiotics used to treat macrolide-susceptible  
347 Streptococcus pyogenes infections may be due to biofilm formation. *Journal of Clinical  
348 Microbiology* **2006**, *44*, 2721-2727.
- 349 6. Vyas, H.K.N.; Proctor, E.-J.; McArthur, J.; Gorman, J.; Sanderson-Smith, M. Current  
350 Understanding of Group A Streptococcal Biofilms. *Current Drug Targets* **2019**, *20*, 982-993,  
351 doi:<http://dx.doi.org/10.2174/1389450120666190405095712>.
- 352 7. Oliver-Kozup, H.; Martin, K.H.; Schwegler-Berry, D.; Green, B.J.; Betts, C.; Shinde, A.V.; Van  
353 De Water, L.; Lukomski, S. The group A streptococcal collagen-like protein-1, Scl1, mediates

- 354 biofilm formation by targeting the extra domain A-containing variant of cellular fibronectin  
355 expressed in wounded tissue. *Mol Microbiol* **2013**, *87*, 672-689, doi:10.1111/mmi.12125.
- 356 8. Lembke, C.; Podbielski, A.; Hidalgo-Grass, C.; Jonas, L.; Hanski, E.; Kreikemeyer, B.  
357 Characterization of biofilm formation by clinically relevant serotypes of group A  
358 streptococci. *Applied and environmental microbiology* **2006**, *72*, 2864-2875.
- 359 9. Sugareva, V.; Arlt, R.; Fiedler, T.; Riani, C.; Podbielski, A.; Kreikemeyer, B. Serotype- and  
360 strain- dependent contribution of the sensor kinase CovS of the CovRS two-component  
361 system to *Streptococcus pyogenes* pathogenesis. *BMC Microbiology* **2010**, *10*, 34,  
362 doi:10.1186/1471-2180-10-34.
- 363 10. Cho, K.H.; Caparon, M.G. Patterns of virulence gene expression differ between biofilm and  
364 tissue communities of *Streptococcus pyogenes*. *Mol Microbiol* **2005**, *57*, 1545-1556,  
365 doi:10.1111/j.1365-2958.2005.04786.x.
- 366 11. Bessen, D.E.; Lizano, S. Tissue tropisms in group A streptococcal infections. *Future Microbiol*  
367 **2010**, *5*, 623-638, doi:10.2217/fmb.10.28.
- 368 12. Vyas, H.K.N.; Indraratna, A.D.; Everest-Dass, A.; Packer, N.H.; De Oliveira, D.M.P.; Ranson,  
369 M.; McArthur, J.D.; Sanderson-Smith, M.L. Assessing the Role of Pharyngeal Cell Surface  
370 Glycans in Group A *Streptococcus* Biofilm Formation. *Antibiotics* **2020**, *9*, 775,  
371 doi:<https://doi.org/10.3390/antibiotics9110775>.
- 372 13. Matysik, A.; Kline, K.A. *Streptococcus pyogenes* capsule promotes microcolony-  
373 independent biofilm formation. *Journal of Bacteriology* **2019**, 10.1128/jb.00052-19, JB.00052-  
374 00019, doi:10.1128/jb.00052-19.
- 375 14. Manetti, A.G.; Zingaretti, C.; Falugi, F.; Capo, S.; Bombaci, M.; Bagnoli, F.; Gambellini, G.;  
376 Bensi, G.; Mora, M.; Edwards, A.M., et al. *Streptococcus pyogenes* pili promote pharyngeal  
377 cell adhesion and biofilm formation. *Mol Microbiol* **2007**, *64*, 968-983, doi:10.1111/j.1365-  
378 2958.2007.05704.x.
- 379 15. Marks, L.R.; Mashburn-Warren, L.; Federle, M.J.; Hakansson, A.P. *Streptococcus pyogenes*  
380 biofilm growth in vitro and in vivo and its role in colonization, virulence and genetic  
381 exchange. *Journal of Infectious Diseases* **2014**, jiu058.
- 382 16. McKay, F.C.; McArthur, J.D.; Sanderson-Smith, M.L.; Gardam, S.; Currie, B.J.; Sriprakash,  
383 K.S.; Fagan, P.K.; Towers, R.J.; Batzloff, M.R.; Chhatwal, G.S., et al. Plasminogen binding by  
384 group A streptococcal isolates from a region of hyperendemicity for streptococcal skin  
385 infection and a high incidence of invasive infection. *Infection and immunity* **2004**, *72*, 364-370,  
386 doi:10.1128/iai.72.1.364-370.2004.
- 387 17. Sanderson-Smith, M.; De Oliveira, D.M.P.; Guglielmini, J.; McMillan, D.J.; Vu, T.; Holien, J.K.;  
388 Henningham, A.; Steer, A.C.; Bessen, D.E.; Dale, J.B., et al. A Systematic and Functional  
389 Classification of *Streptococcus pyogenes* That Serves as a New Tool for Molecular Typing  
390 and Vaccine Development. *The Journal of infectious diseases* **2014**, *210*, 1325-1338,  
391 doi:10.1093/infdis/jiu260 %J The Journal of Infectious Diseases.
- 392 18. Aziz, R.K.; Pabst, M.J.; Jeng, A.; Kansal, R.; Low, D.E.; Nizet, V.; Kotb, M. Invasive MIT1  
393 group A *Streptococcus* undergoes a phase-shift in vivo to prevent proteolytic degradation of  
394 multiple virulence factors by SpeB. **2004**, *51*, 123-134, doi:10.1046/j.1365-2958.2003.03797.x.

- 395 19. Marks, L.R.; Parameswaran, G.I.; Hakansson, A.P. Pneumococcal interactions with epithelial  
396 cells are crucial for optimal biofilm formation and colonization in vitro and in vivo. *Infect*  
397 *Immun* **2012**, *80*, 2744-2760, doi:10.1128/iai.00488-12.
- 398 20. Williams, D.L.; Bloebaum, R.D. Observing the biofilm matrix of *Staphylococcus epidermidis*  
399 ATCC 35984 grown using the CDC biofilm reactor. *Microscopy and Microanalysis* **2010**, *16*, 143-  
400 152.
- 401 21. Christensen, G.D.; Simpson, W.; Younger, J.; Baddour, L.; Barrett, F.; Melton, D.; Beachey, E.  
402 Adherence of coagulase-negative staphylococci to plastic tissue culture plates: a quantitative  
403 model for the adherence of staphylococci to medical devices. *Journal of clinical microbiology*  
404 **1985**, *22*, 996-1006.
- 405 22. Wilson, C.; Lukowicz, R.; Merchant, S.; Valquier-Flynn, H.; Caballero, J.; Sandoval, J.;  
406 Okuom, M.; Huber, C.; Brooks, T.D.; Wilson, E., et al. Quantitative and Qualitative  
407 Assessment Methods for Biofilm Growth: A Mini-review. *Res Rev J Eng Technol* **2017**, *6*,  
408 [http://www.rruj.com/open-access/quantitative-and-qualitative-assessment-methods-for-](http://www.rruj.com/open-access/quantitative-and-qualitative-assessment-methods-for-biofilm-growth-a-minireview-.pdf)  
409 [biofilm-growth-a-minireview-.pdf](http://www.rruj.com/open-access/quantitative-and-qualitative-assessment-methods-for-biofilm-growth-a-minireview-.pdf).
- 410 23. Pantanella, F.; Valenti, P.; Natalizi, T.; Passeri, D.; Berlutti, F. Analytical techniques to study  
411 microbial biofilm on abiotic surfaces: pros and cons of the main techniques currently in use.  
412 *Annali di igiene : medicina preventiva e di comunita* **2013**, *25*, 31-42, doi:10.7416/ai.2013.1904.
- 413 24. Azeredo, J.; Azevedo, N.F.; Briandet, R.; Cerca, N.; Coenye, T.; Costa, A.R.; Desvaux, M.; Di  
414 Bonaventura, G.; Hébraud, M.; Jaglic, Z., et al. Critical review on biofilm methods. *Critical*  
415 *Reviews in Microbiology* **2017**, *43*, 313-351, doi:10.1080/1040841X.2016.1208146.
- 416 25. Barthelson, R.; Mobasser, A.; Zopf, D.; Simon, P. Adherence of *Streptococcus pneumoniae*  
417 to respiratory epithelial cells is inhibited by sialylated oligosaccharides. *Infection and*  
418 *immunity* **1998**, *66*, 1439-1444.
- 419 26. Frick, I.M.; Schmidtchen, A.; Sjobring, U. Interactions between M proteins of *Streptococcus*  
420 *pyogenes* and glycosaminoglycans promote bacterial adhesion to host cells. *European journal*  
421 *of biochemistry* **2003**, *270*, 2303-2311, doi:10.1046/j.1432-1033.2003.03600.x.
- 422 27. Ryan, P.A.; Juncosa, B. Group A streptococcal adherence. **2016**.
- 423 28. Ryan, P.A.; Pancholi, V.; Fischetti, V.A. Group A streptococci bind to mucin and human  
424 pharyngeal cells through sialic acid-containing receptors. *Infect Immun* **2001**, *69*, 7402-7412,  
425 doi:10.1128/iai.69.12.7402-7412.2001.
- 426 29. McDougald, D.; Rice, S.A.; Barraud, N.; Steinberg, P.D.; Kjelleberg, S. Should we stay or  
427 should we go: mechanisms and ecological consequences for biofilm dispersal. *Nature reviews.*  
428 *Microbiology* **2012**, *10*, 39-50, doi:10.1038/nrmicro2695.
- 429 30. Gjermansen, M.; Ragas, P.; Sternberg, C.; Molin, S.; Tolker-Nielsen, T. Characterization of  
430 starvation-induced dispersion in *Pseudomonas putida* biofilms. *Environmental Microbiology*  
431 **2005**, *7*, 894-904, doi:10.1111/j.1462-2920.2005.00775.x.
- 432